Modeling of Critical Current Density of Bulk High T_c Superconductors

M. Santosh*
St. Mary International School, 1-16-19, Seta, Setagaya-ku, Tokyo 158-8668, Japan

(Received February 3, 2014; in final form May 5, 2014)

Magnetic field dependence of critical current density (J_c) of $ErBa_2Cu_3O_y$ thick film "Er-123" and melt textured $GdBa_2Cu_3O_y$ bulk "Gd-123" at liquid nitrogen temperature is reported. Gd-123 exhibits a usual peak effect at magnetic fields around 2 T, while J_c of the Er-123 thick film continuously decreases with increasing field. The model of thermally activated flux motion was adopted to fit the critical current density of both Gd-123 and Er-123 materials. It was found that the critical current density of both types of the high T_c materials could be modeled by the model of thermally activated flux motion utilizing a combination of two functions; one increasing and another one decreasing with field.

DOI: 10.12693/APhysPolA.126.808
PACS: 74.72.–h; 74.25.Sv; 74.20.–z

1. Introduction

Top seeded melt-processed $LREBa_2Cu_3O_y$ "LRE-123" (light rare earth, LRE = Sm, Nd, Eu, Gd) compounds are prominent materials for permanent superconducting magnets [1]. Recent progress in the technology has notably improved their electromagnetic performance, brought an essential breakthrough in mechanical performance, and significantly reduced the fabrication cost [2]. As a result, bulk high-T_c superconducting magnets have established a new era of engineering applications as a compact source of magnetic field. Such magnets can be employed in superconducting electric motors, flywheel energy storage systems, compact devices of magnetic resonance imaging (MRI) and nuclear magnetic resonance (NMR), water purification systems, and/or various kinds of superconducting magnets in research and development. According to the latest reviews [3–5], some of them are ready to launch market in a close future. For exampl, Hitachi Ltd., Japan, recently developed and designed a mobile combined membrane and a magnetic separator, employing long high-T_c bulk superconductors, for a quick removal of phytoplankton procreating in high amounts in eutrophic lakes and dams [6]. In water cleaning tests with kaolin as a pollution source the water cleaning efficiency was found better than 90%. Another important and challenging application is HTS Maglev being under study and development by Central Japan Railways, Japan in cooperation with Southwest Jiao Tong University, China [7].

As a part of an internship program at Shibaura Institute of Technology (SIT), Tokyo, and in a school science fair project, I studied properties of superconductors related to levitation, guidance forces etc. [8]. I prepared melt-textured $YBa_2Cu_3O_y$ material and characterized it for use as a permanent magnet [9]. In the technological and characterization process the differential thermal analysis (DTA), X-ray difractometry (XRD), optical microscopy, and levitation force measurement techniques were used to characterize the material. Further, the materials' microstructure was investigated by scanning electron microscope.

Selection and fabrication of materials appropriate for use in high magnetic fields is crucial for industrial applications. In this project, we selected and fabricated in SIT Gd-123 melt-processed material and Er-123 thick film and performed magnetization measurements at 77 K of them. From the magnetic data the critical current density was estimated. The $J_c(B)$ curves were modeled in terms of the thermally activated flux creep model described below.

2. Magnetization experiments

Magnetization hysteresis loops (MHLs) were measured at 77 K using a commercial SQUID magnetometer (Quantum Design, model MPMS7). For this study, small samples of the dimensions: Gd-123: $1.43 \times 2.54 \times 0.63$ mm^3 and Er-123: $2.36 \times 2.74 \times 0.0075$ mm^3 were used. From the obtained data the critical current density, J_c, was estimated using the extended Bean critical state model [10],

$$J_c = 20\Delta m/[a^2 d(b - a/3)], \quad (1)$$

where d is thickness, a, b are transverse dimensions of the sample, $b \geq a$, and Δm is the difference of magnetic moments on the descending and ascending field branch of the MHL, respectively. The magnetization curves of the measured samples are in Fig. 1: the Er-123 thick film (left) and the Gd-123 bulk (right). Both curves are also slightly rotated upwards, due to paramagnetism of Er and Gd ions. If we take the linear paramagnetic background as a basis, the general trend of the superconducting, irreversible part is in both cases that the magnetic

*e-mail: santoshjuly@msn.com

moment decreases with increasing magnetic field. In Gd-123 the magnetic moment exhibits one more feature at intermediate fields, so called second peak. The magnetic moment there increases with magnetic field and decreases thereafter. It is even better seen on the field dependence of the critical current density, $J_c(B)$, Fig. 2.

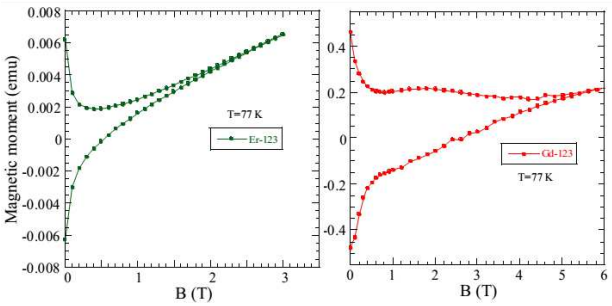

Fig. 1. Field dependence of magnetic moment, measured by SQUID at 77 K, for the $ErBa_2Cu_3O_y$ thick film (left) and $GdBa_2Cu_3O_y$ bulk superconductor (right).

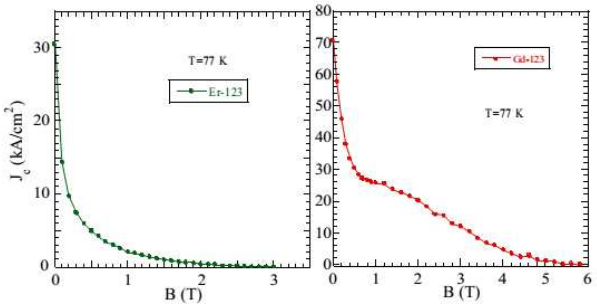

Fig. 2. Field dependence of the critical current density for the $ErBa_2Cu_3O_y$ thick film (left) and $GdBa_2Cu_3O_y$ bulk superconductors (right) at 77 K.

3. Modeling the critical current density curves

Several models have been suggested to describe vortex pinning effects in superconductors and the associated shape of the magnetization curve, most of them for classical superconductors. The assumptions used for development of classical models, however, usually fail in the case of high-T_c materials. Based on the thermodynamic and some phenomenological considerations for bulk high-T_c superconductors with thermally activated flux motion of Perkins et al. [11, 12], Jirsa et al. proposed a formula that enables to fit the magnetic data and the associated critical current density as a function of magnetic field [13]. The $J_c(B)$ shape in bulk RE-123 superconductors can be described as a combination of two overlapping peaks. The first peak exponentially decays with increasing magnetic field, the second one exhibits maximum at intermediate fields. The first peak can be expressed as [13]:

$$y = A_1 \exp(-B/B_0), \tag{2}$$

where A_1 is a constant equal to the height of the peak, B stands for the applied magnetic field value, and B_0 is a fitting constant indicating how fast the peak decays with increasing field.

In accord with the common behavior of superconducting thin films, also the magnetic data of the Er-123 thick film exhibited only a single central peak (see Fig. 2, left). We tried to model the curve by Eq. (2), where we set $B_0 = 0.5$ T as the first guess and fixed A_1 at the experimental value $J_c(0) = 30.535$ kA/cm^2. For a series of B_0 values the model curves are shown in Fig. 3, left. The best fit (not much satisfactory) was obtained for $J_c(B) = 30.535\exp(-B/0.18)$ with J_c in kA/cm^2 and B in T.

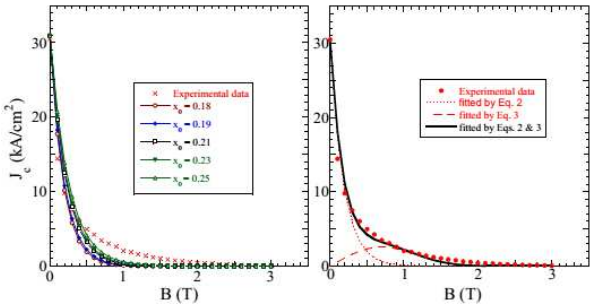

Fig. 3. Left: the experimental data (crosses) for Er-123 thick film fitted by Eq. (2). Right: the same experimental data fitted by combined Eqs. (2) and (3).

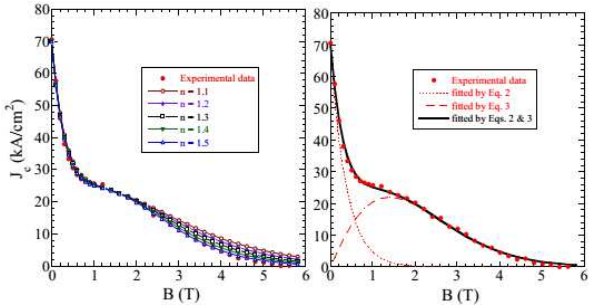

Fig. 4. The experimental data (symbols) were fitted by Eqs. (2) and (3) (the full lines) for Gd-123 bulk data.

In bulk high-T_c superconductors usually a second peak or at least a shoulder appears on the experimental curve at intermediate fields. Modeling of this peak requires use of a combination of two functions, one *increasing* and another one *decreasing* with field. The following formula fulfills these requirements [11–13]:

$$y = A_2(B/B_m)\exp([1-(B/B_m)^n]/n). \tag{3}$$

A_2 is in general height of the second peak. The more separated this peak from the first one, the closer is the A_2 value to the real height of the second peak. In practice, A_2 is always little bit lower, but the peak height is a good

first choice. B_m represents position of the second peak or of the shoulder on the experimental curve; we can find it (approximately) from the measured data. n value lies always between 1 and 3, in most cases around 2. For the first guess we chose 2.

We found the following best fit for Gd-123 system (with sum of Eqs. (2) and (3)): $J_c = 70.0\exp(-B/0.37) + 22.0(B/1.4)\exp([1-(B/1.4)^{1.5}]/1.5)$ with J_c in kA/cm^2 and B in Tesla. The resulting curve is shown in Fig. 4. The fit is usually done by means of a commercial fitting program but it can be done also by hand, though not so precisely. The left figure illustrates how variation of one of the parameters, n, affects the curve shape. How good the fit can be, it is shown in Fig. 4 right. There, the two dotted curves are the individual contributions, Eqs. (2) and (3), and the solid curve is their sum. One can see in Fig. 4 that the function fitting the first peak decays rather fast and turns to zero in high magnetic fields. There, on the other hand, the second function dominates and fully fits the experimental data. Only in the intermediate field range the functions cooperate and their combination fits the experiment. Slope of the high-field part of the data is fully controlled by parameter n (see Fig. 4, left). The lower its value, the slower the curve decays. In the Er-123 data (Fig. 3) the second peak is not for the first glance obvious. However, trying to fit the experimental curve by the single function (2) was not satisfactory for any value of B_0. Although the contribution of the mechanism associated with pinning by point-like defects (second peak) is very weak in the Er-123 thick film sample, it still significantly affects the form of the experimental curve at high magnetic fields. The best fit for the Er-123 material is shown in Fig. 3, right. It is given by $J_c(B) = 30.53\exp(-B/0.18) + 2.6B/0.7\exp([1-(B/0.7)^{2.5}]/2.5)$ with J_c in kA/cm^2 and B in Tesla. In bulk RE-123 materials, two main sources of point-like defects have been identified, namely (i) oxygen vacancies [14] in YBaCuO and all other cuprates and (ii) the LRE/Ba ions substitutions in LRE-123 compounds [15]. As Er is not a LRE, only oxygen vacancies are the most probable source of the J_c enhancement at intermediate and high magnetic fields in Er-123 thick films.

4. Summary

The critical current density of Er-123 and Gd-123 materials was estimated for liquid nitrogen temperature, 77.3 K, using magnetization measurements on SQUID magnetometer. The results indicate that Gd-123 material can be used for high-field applications, in contrast to the Er-123 thick film. It is partially caused by not yet fully optimized technology of Er-123 thick films. Model of thermally activated flux motion was utilized to model the critical current density of both materials. It worked well for both compounds and both samples' forms, bulk and thick film. In the latter case, the experimental curve shape fit was not good with a simple exponential decay as commonly observed in thin RE-123 films; an additional term was needed to model the high-field part of the curve. We used the term describing in bulk samples fishtail peak or shoulder, attributed in literature to the action of point-like defects or their clusters. This weak second term in the Er-123 thick film was ascribed to a small amount of oxygen vacancies.

Acknowledgments

I would like to thank Mr. Kagei, Headmaster, Miss Ramseys, high school principal, Brother Deo, English teacher, Mr. McGuire, biology teacher, Mr. Ochola, chemistry teacher, Mr. Aaron Ragon Counselor at St. Mary's International School for helpful discussions and constant encouragement of the projects (including science fair). Special thanks belong to Dr. Milos Jirsa (Institute of Physics, ASCR) for his valuable suggestions, advising the project and checking the manuscript. Finally, I would like to thank Prof. M. Murakami, President of Shibaura Institute of Technology (SIT), for providing me the HTSc materials and giving me opportunity to work at SIT.

References

[1] M. Murakami, N. Sakai, T. Higuchi, S.I. Yoo, *Supercond. Sci. Technol.* **9**, 1015 (1996).

[2] M. Tomita, M. Murakami, *Nature* **421**, 517 (2003).

[3] J.R. Hull, *Supercond. Sci. Technol* **13**, R1 (2001).

[4] T. Ohara, H. Kumakura, H. Wada, *Physica C* **13**, 1272 (2001).

[5] A.C. Day, M. Strasik, K.E. McCrary, P.E. Johnson, J.W. Gabrys, J.R. Schindler, R.A. Hawkins, D.L. Carlson, M.D. Higgins, J.R. Hull, *Supercond. Sci. Technol.* **15**, 838 (2002).

[6] H. Hayashi, N. Nagabuchi, N. Sahi, T. Mizumori, K. Sano, *Physica C* **412-414**, 766 (2004).

[7] Y. Zhao, J.S. Wang, S.Y. Wang, Z.Y. Ren, H.H. Song, X.R. Wang, C.H. Cheng, *Physica C* **412-414**, 771 (2004).

[8] M. Santosh, M.R. Koblischka, *J. Phys. Educat.* (2013), communicated.

[9] M. Santosh, *Summer Internship Report*, submitted to *SIT*, 2012.

[10] D X. Chen, R.B. Goldfarb, *J. Appl. Phys.* **66**, 2489 (1989).

[11] G.K. Perkins, L.F. Cohen, A.A. Zhukov, A.D. Caplin, *Phys. Rev. B* **51**, 8513 (1995).

[12] G.K. Perkins, A.D. Caplin, *Phys. Rev. B* **54**, 12551 (1996).

[13] M. Jirsa, L. Půst, D. Dlouhý, M.R. Koblischka, *Phys. Rev. B* **55**, 3276 (1997).

[14] H. Küpfer, Th. Wolf, C. Lessing, A.A. Zhukov, X. Lançon, R. Meier-Hirmer, W. Schauer, H. Wühl, *Phys. Rev. B* **58**, 2886 (1998).

[15] N. Chikumoto, J. Yoshioka, M. Murakami, *Physica C* **291**, 79 (1997).